Rare Metal Materials and Engineering
Volume 38, Issue 4, April 2009
Online English edition of the Chinese language journal

Available online at www.sciencedirect.com

ScienceDirect

Cite this article as: Rare Metal Materials and Engineering, 2009, 38(4): 0574–0578.

ARTICLE

Microstructure and Mechanical Properties of Laser Solid Formed Ti-6Al-4V from Blended Elemental Powders

Tan Hua, Chen Jing, Zhang Fengying, Lin Xin, Huang Weidong

State Key Laboratory of Solidification Processing, Northwestern Polytechnical University, Xi'an 710072, China

Abstract: The microstructure and mechanical properties of laser solid formed Ti-6Al-4V from the blend of Ti, Al, and V powders were investigated. It is found that the macrostructure changes from equiaxed to columnar grains with the increase of the laser power, which is very different from that of the samples using pre-alloyed powders as cladding materials. The disturbance effect of the mixing enthalpy during laser deposition is considered responsible for the formation of equiaxed grains at low laser powers. The microstructure within prior-β grains mainly consists of Widmanstätten α laths separated by β-Ti, which is basically identical to those from pre-alloyed powders. Oxygen content of as-deposited samples was measured and the tensile testing was carried out. The results show that the oxygen content of as-deposited Ti-6Al-4V from blended elemental powders is only about 0.1wt.% and the mechanical properties are comparable to or even better than that of conventionally wrought material.

Key words: blended elemental powders; laser solid forming; Ti-6Al-4V; microstructure; mechanical properties

Laser solid forming (LSF) is a solid freeform fabrication method which can be used to manufacture near-net shape metallic components directly from CAD files[1]. In the process of LSF, powder is fed into a molten pool created by a laser beam, and some are built in point-by-point and layer-by-layer fashion. LSF is particularly attractive for the fabrication of titanium aerospace components because it has many outstanding advantages, e.g., a component can be fabricated rapidly without using a mold. Thus, much recent efforts have been conducted to develop titanium LSF processes. P A Kobryn et al investigated the effects of processing parameters on microstructure, porosity, and build height of LSF Ti-6Al-4V[2]. Xinhua Wu et al established a finite element model to predict the thermal histories of LSF Ti-6Al-4V thin wall samples to correlate the process parameters with the microstructure of Ti-6Al-4V[3]. S M KELLY et al developed a microstructure evolution map to qualitatively determine the equilibrium and non-equilibrium phase transformations during LSF of Ti-6Al-4V[4,5]. Xue Lei et al investigated the feasibility of laser rapid repairing on the aircraft components of Ti-6Al-4V alloy[6].

Generally, the pre-alloyed powders are used as the deposited materials in the process of LSF. However, since the powders are injected into the molten pool synchronously and experience re-melting and re-solidification process, we can deposit a blend of elemental powders and create an alloy in situ by LSF, which could potentially reduce the processing costs by a large extent. LSF from blended elemental powders is also a powerful tool to investigate new alloy systems and create innovative materials. In addition, by controlling the mixing process of the powders from several powder feeders, graded compositions within the same sample can be obtained more flexibly. In fact, a number of studies have been conducted on LSF of titanium alloys from blended elemental powders. H L Fraser et al used this approach to study the laser deposited compositionally graded α/β titanium- vanadium alloys, titanium-molybdenum alloys, metallic biomaterials, Ti-TiB and so on[7-12]. However, most of the previous studies focused on investigating the effect of compositional changes on phase transformation during LSF of titanium alloys, and limited work was concerned with the morphology of the prior-β grains.

Received date: July 28, 2008
Foundation items: National Natural Science Foundation of China (No. 50871089); Talent Cultivating Program of Northwestern Polytechnical University (Grant No.05XE0131); National Basic Research Program ("973" Program) of China (No. 2007CB613805); Program for New Century Excellent Talents in University of China (Grant No.NCET-06-0879).
Biography: Tan Hua, Candidate for Ph. D., State Key Laboratory of Solidification Processing, Northwestern Polytechnical University, Xi'an 710072, P. R. China, Tel: 0086-29-88492884-801, E-mail: tannwpu@gmail.com.

In addition, few studies reported on LSF of Ti-6Al-4V by this method. The present work was undertaken to examine the microstructure characteristics and mechanical properties of LSF Ti-6Al-4V from blended elemental powders. The microstructural differences found in Ti-6Al-4V deposited from blended elemental powders and from pre-alloyed powders were mainly discussed.

1 Experimental

Commercially pure Ti, Al, and V powders were used as the deposited materials, and the powder characteristics are listed in Table 1. The powders were dried in a vacuum oven for 24 h and then mixed in a ball grinder for 2 h. The substrates were pure Ti sheets with dimensions of 100 mm×50 mm×10 mm.

Table 1 Characteristics of the powders

Powder	Particle appearance	Particle size/μm	Oxygen content/wt.%
Ti	Spherical	100-150	0.069
Al	Spherical	60-100	0.080
V	Irregular	60-100	0.071

The samples were fabricated using a LSF system consisting of a 5 kW continuous wave CO_2 laser from Rofin Sinar, a four-axis numerical control work table, and a powder feeder with a coaxial nozzle. The experiments were conducted inside a glove box filled with argon gas. A schematic illustration of the LSF system is presented in Fig. 1. During the LSF process, the laser beam was directed onto the substrate to create a molten pool into which the premixed powders were injected through the coaxial nozzle. Thin wall samples of 50 mm×12 mm×3 mm and the tensile samples of 100 mm×30 mm×3 mm were fabricated. The processing parameters are given in Table 2.

The microstructure of the deposits was characterized by an optical microscope and a scanning electron microscope (SEM). The oxygen content of the powders and the deposits were measured using an inductively coupled plasma atomic emission spectrometer (ICP-AES). The mechanical properties were tested on an INSTRON11-96 electronic tensile machine.

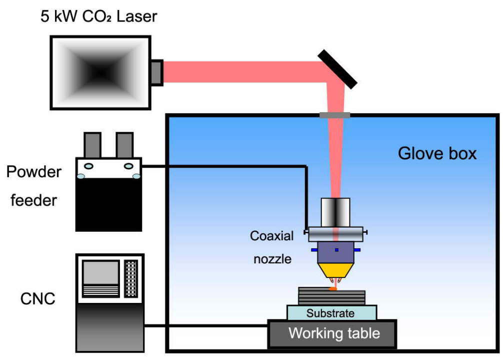

Fig.1 Schematic of experimental apparatus

Table 2 Processing parameters of the LSF route

Laser power/ W	Scanning velocity/ $mm \cdot s^{-1}$	Diameter of spot size/mm	Powder feeding rate/$g \cdot min^{-1}$	Shielding gas flow/ $L \cdot min^{-1}$
1250-2300	4.5	3.0	4.5	6

2 Results and Discussion

2.1 Macro- and microstructure

Fig.2 shows the typical morphologies of LSF Ti-6Al-4V from blended elemental powders at a range of laser powers for a given scanning velocity. It is seen that the macrostructure changes from equiaxed to columnar grains with the increase of the laser power (Fig.2a-2c). At a low laser power of 1250 W, equiaxed grains with an average grain size of 500-1000 μm dominate in the most regions of the sample, as shown in Fig.2a. At a higher laser power of 1850 W, columnar grains are formed at the upper side and begin to grow epitaxially at almost half part of the sample, whose sizes are much larger than those of equiaxed grains formed at the bottom (Fig.2b). At the highest laser power of 2300 W, the sample is dominated by the columnar grains entirely, and only some small sizes of equiaxed grains (with an average grain size of 150 μm) exist at the top (Fig.2c and 2d). By high magnification microscopic view, a few small sizes of columnar grains can be seen at the very bottom of all the samples. The height of this region is normally less than three deposited layers at the laser powers of 1250 W and 1850 W, and then the columnar to equiaxed transition (CET) occurs, shown clearly in Fig.2e.

The influence of the processing parameters on the grain morphology of LSF Ti-6Al-4V has been investigated in our earlier work[13] and it has been found the macrostructure changes from columnar grains to equiaxed grains with the increasing of laser power at a given scanning velocity. However, the macrostructure of the deposits obtained from blended elemental powders is very different from that of samples using pre-alloyed powders as deposited materials. In order to understand the observed macrostructure evolution, the conditions under which CET will occur for Ti-6Al-4V were obtained by Lin's model[14] and are presented in Fig.3. The fixed-point molten pool temperature measurement[15] was also carried out to obtain the solidification conditions at the tail of the molten pool. Fig.4 shows the cooling curve, measured by a two-color infrared thermometer, of a specific position on the sample obtained with 1250 W laser power and 7.5 mm/s laser scanning velocity. The liquidus temperature calculated by Thermal-Calc is marked by the dashed line. Considering that the solidification velocity at the tail of the molten pool approximately equals to the scanning velocity, the temperature gradient G and solidification velocity V_S at the tail of the molten pool can be obtained as 2.9×10^5 K/m and 7.5 mm/s, respectively. Similarly, the solidification parameters at the tail of the molten pool at laser powers of 1850 W and 2300 W were also ob-

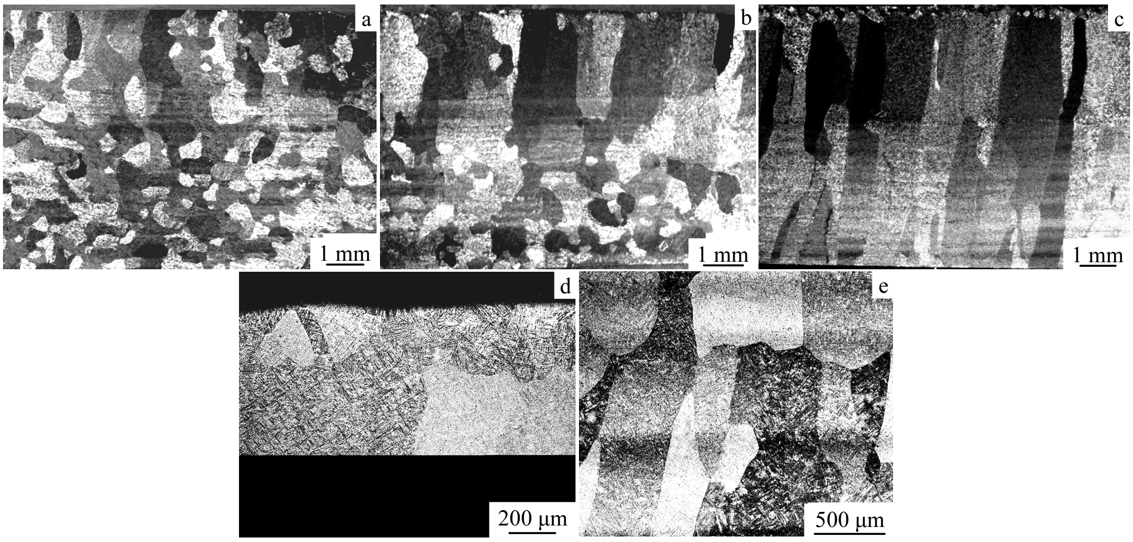

Fig.2 Micrographs of LSF Ti-6Al-4V from blended elemental powders at a scanning velocity of 7.5 mm/s and at a range of laser powers: (a) 1250 W, (b) 1850 W, (c) 2300 W, (d) the top of the sample obtained at 2300 W, and (e) the bottom of the sample obtained at 1250 W

tained, as presented in Fig. 3. Since the tail of the molten pool is most vulnerable to the occurrence of CET[12], it is clear that fully columnar morphology should be obtained at low laser powers of 1250 W and 1850 W under the processing parameters used in this study (Fig.3). The results also suggest that increasing of laser power at a given scanning velocity tends to promote the occurrence of CET. It can be concluded that the evolution of the grain morphology obtained using pre-alloyed powders[11] agrees well with the theoretical predictions while the macrostructure of the deposits obtained from blended elemental powders (Fig.2) are very different from the theoretical predictions at low laser powers (Fig.3). At low laser powers, potential nuclei may be added to the molten pool since some large powder particles may not fully melt and they can serve as nuclei to promote the formation of equiaxed grains. However, few unmelted particles were found in the microstructure of all the deposits obtained from blended elemental powders in this study. According to the analysis mentioned above, it can be deduced that the mixing enthalpy of the elements in the molten pool is an important factor during LSF from blended elemental powders. By Miedema's theory[16], the mixing enthalpy of Ti-6Al-4V was calculated out to be –11.35 kJ/mol. As known, the crystal growth direction is affected severely by the direction of the heat flow. Since the intermixing of Ti, Al, and V in the molten pool is exothermic, it is appropriate to consider that the liberated heat may lead to the change of the heat flow direction in the local area ahead of the solid/liquid interface, i.e., when the next layer is deposited, the disturbance of the heat flow can interrupt the epitaxial growth of the columnar grains along the deposit direction and promote the nucleation and growth of the new grains ahead of the solid/liquid interface, thus resulting in the formation of irregularly equiaxed grains at low laser powers. With an increase of laser power, the relative effect of the heat disturbance is weakened, so the β-Ti columnar grains are formed and grow epitaxially (Fig.2c). It also can be inferred that increasing of the laser power further, the grain morphologies will change from columnar grains to equiaxed grains again according to the theoretical predictions (experiment was not carried out because too high laser power may lead to the evaporation loss of some element). In addition, the temperature gradient G is the highest near the substrate, thus contributing to the formation of columnar grains with smaller sizes at the very bottom of all the samples.

Fig.5 reveals the microstructure in prior β-Ti grains of as-deposited Ti-6Al-4V from blended elemental powders. As can be seen, the microstructure within prior β grains mainly consists of Widmanstätten α laths with the thickness less than 2 μm separated by β-Ti, which is basically identical to those from pre-alloyed powders as reported previously[17].

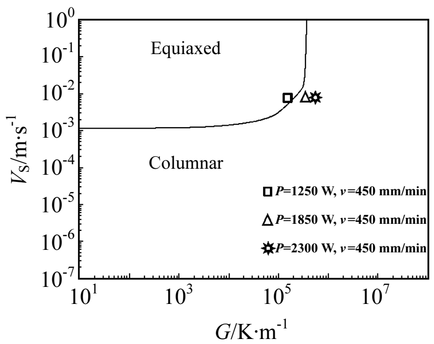

Fig.3 CET profile showing the regions of columnar dendrites and equiaxed dendrites as a function of temperature gradient G and solidification velocity V_S

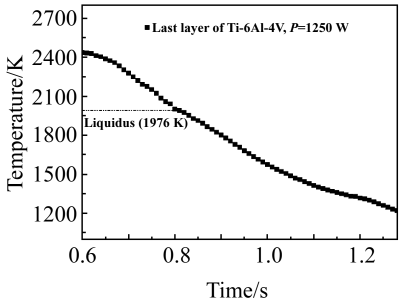

Fig.4 Cooling curve of the LSF Ti-6Al-4V from blended elemental powders obtained with 1250 W laser power and 7.5 mm/s laser scanning velocity

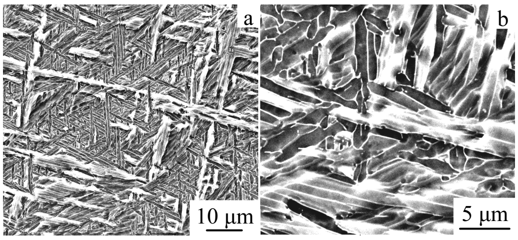

Fig.5 SEM micrographs of the microstructure in prior-β grains: (a) low magnification image; (b) high magnification image

2.2 Mechanical properties

The room-temperature tensile properties of as-deposited Ti-6Al-4V from blended elemental powders are illustrated in Fig.6. It should be noted that the data were obtained by averaging the mechanical properties of the samples manufactured with different laser powers. For comparison, the data of those obtained from pre-alloyed powders with different oxygen content, and the data of wrought material (ASTM B381-05) are also included. A comparison of the properties for LSF Ti-6Al-4V with different oxygen content reveals that a decrease in oxygen content will lead to some decrease in strength and a substantial increase in ductility. It is in a good agreement with the well known influence of oxygen content on the properties of titanium alloys[18]. Ultimate strength, yield strength, and elongation of as-deposited Ti-6Al-4V from blended elemental powders are 970 MPa, 870 MPa, and 13.0%, respectively, which surpass ASTM limits (895 MPa, 825 MPa and 10.0%). Fig.7 shows the SEM micrographs of the fracture surface for as-deposited Ti-6Al-4V from blended elemental powders, which is characterized by the larger and deeper dimples. The results clearly indicate that a good combination of strength and ductility for LSF Ti-6Al-4V from blended elemental powders can be obtained. It might be ascribed to the low oxygen content (below 0.10 wt.%) in elemental powders and fine size microstructure in deposit.

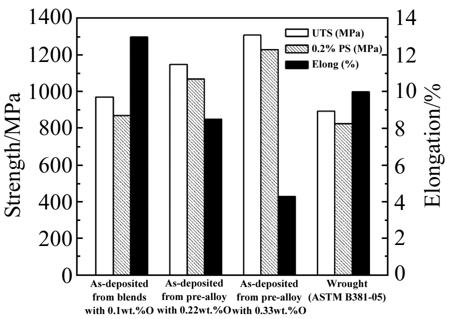

Fig.6 Room temperature tensile properties of LSF Ti-6Al-4V

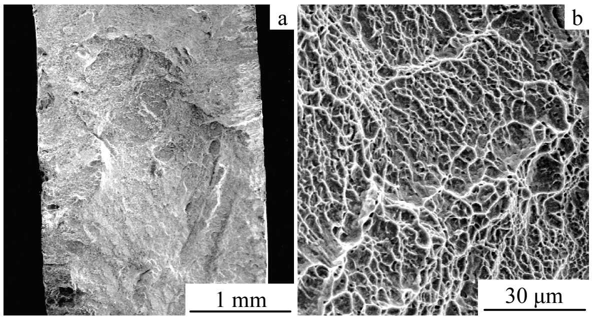

Fig.7 SEM micrographs of the fracture surface for as-deposited Ti-6Al-4V from blended elemental powders: (a) macroscopic fractograph and (b) microscopic fractograph

3 Conclusions

The macrostructure of the deposits changes from irregularly equiaxed grains to columnar grains with increasing of laser power. The formation of the irregularly equiaxed grains at low laser powers is mainly attributed to the disturbance effect of the mixing enthalpy. The microstructure within prior-β grains mainly consists of Widmanstätten α laths with a certain volume fraction of β-Ti. The room-temperature mechanical properties of as-deposited Ti-6Al-4V from blended elemental powders exceed those of conventionally wrought material.

References

1 Huang Weidong(黄卫东), Lin Xin(林 鑫), Chen Jing(陈 静) *et al*. *Laser Solid Forming Technology*(激光立体成形)[M]. Xi'an: Northwestern Polytechnical University Press, 2007: 1
2 Kobryn P A, Moore E H, Semiatin S L. *Scripta Mater*[J], 2000, 43: 299
3 Qian L, Mei J, Liang J *et al*. *J Mater Sci Technol*[J], 2005, 21: 597
4 Kelly S M, Kampe S L. *Metall Mater Trans A*[J], 2004, 35: 1861
5 Kelly S M, Kampe S L. *Metall Mater Trans A*[J], 2004, 35: 1869
6 Xue Lei(薛 雷), Chen Jing(陈 静), Zhang Fengying(张凤英) *et al*. *Rare Metal Mat Eng*(稀有金属材料与工程)[J], 2006, 35(11): 1817
7 Collins P C, Banerjee R, Banerjee S *et al*. *Mat Sci Eng A*[J], 2003, 352: 118
8 Banerjee R, Collins P C, Bhattacharyya D *et al*. *Acta Mater*[J], 2003, 51: 3277
9 Genç A, Banerjee R, Hill D *et al*. *Mater lett*[J], 2006, 60: 859
10 Nag S, Banerjee R, Fraser H L. *Acta Biomater*[J], 2007, 3: 369

11 Banerjee R, Bhattacharyya D, Collins P C *et al*. *Acta Mater*[J], 2004, 52: 377
12 Banerjee R, Nag S, Fraser H L. *Mat Sci Eng C*[J], 2005, 25: 282
13 Zhang Shuangyin(张霜银), Lin Xin(林 鑫), Chen Jing(陈 静) *et al*. *Rare Metal Mat Eng*(稀有金属材料与工程)[J], 2007, 36(10): 1839
14 Lin X, Yue T M, Yang H O *et al*. *Mat Sci Eng A*[J], 2005, 391: 325
15 Tan Hua, Chen Jing, Lin Xin *et al*. *Mater Sci Forum*[J], 2007, 546-549: 2301
16 Zhang Bangwei(张邦维). *Theory of Embedded Atom Method and Its Application to Materials Science: Atomic Scale Materials Design Theory*(嵌入原子方法理论及其在材料科学中的应用：原子尺度材料设计理论)[M]. Changsha: Hunan University Press, 2003
17 Zhang Shuangyin(张霜银), Lin Xin(林 鑫), Chen Jing(陈 静) *et al*. *Rare Metal Mat Eng*(稀有金属材料与工程)[J], 2007, 36(7): 1263
18 Tao Chunhu(陶春虎), Liu Qingquan(刘庆瑔), Cao Chunxiao(曹春晓) *et al*. *Failure and Prevention of Aeronautical Titanium Alloy*(航空用钛合金的失效及其预防)[M]. Beijing: National Defense Industry Press, 2002

混合元素法激光立体成形 Ti-6Al-4V 的组织及性能研究

谭 华，陈 静，张凤英，林 鑫，黄卫东

(西北工业大学 凝固技术国家重点实验室，陕西 西安 710072)

摘 要：以 Ti、Al、V 混合元素粉末为原料激光沉积 Ti-6Al-4V，并对沉积态试样的组织演化及力学性能进行研究。结果表明，与采用预合金 Ti-6Al-4V 粉末为原料所获得的沉积试样的凝固组织特征有所不同，采用混合元素粉末为原料获得的沉积试样的凝固组织随激光功率的提高逐渐由等轴晶转化为柱状晶，熔池内合金化过程所产生的混合热的扰动作用是导致低功率条件下等轴晶形成的原因。原始 β 晶粒内的微观组织由大量的魏氏 α 板条和一定体积分数的板条间 β 相组成。这与采用预合金粉末基本相同。混合元素法激光立体成形 Ti-6Al-4V 的氧含量仅约 0.1wt.%，沉积态 Ti-6Al-4V 的室温拉伸性能超过锻件标准要求。

关键词：混合元素粉末；激光立体成形；Ti-6Al-4V；组织；性能

作者简介：谭 华，男，1979 年生，博士生，西北工业大学 凝固技术国家重点实验室，陕西 西安 710072，电话：029-88492884-802，E-mail: tannwpu@gmail..com